

Time-Resolved Picosecond Photocurrents in Contacted Carbon Nanotubes

Leonhard Prechtel,[†] Li Song,[‡] Stephan Manus,[‡] Dieter Schuh,[§] Werner Wegscheider,^{||} and Alexander W. Holleitner^{*,†}

[†]Walter Schottky Institut and Physik-Department, Technische Universität München, Am Coulombwall 4, D-85748 Garching, Germany, [‡]Fakultät für Physik and Center for NanoScience (CeNS), Ludwig-Maximilians-Universität, Geschwister-Scholl-Platz 1, D-80539 München, Germany, [§]Institut für Experimentelle und Angewandte Physik, Universität Regensburg, D-93040 Regensburg, Germany, and ^{||}Laboratorium für Festkörperphysik, HPF E 7, ETH Zürich, Schafmattstrasse 16, 8093 Zürich, Switzerland

ABSTRACT We introduce coplanar stripline circuits to resolve the ultrafast photocurrent dynamics of freely suspended carbon nanotubes (CNTs) in the time domain. By applying an on-chip pump–probe laser spectroscopy, we demonstrate that CNTs, contacted by metal electrodes, exhibit a picosecond photocurrent response. We find a combination of an optically induced ultrafast displacement current, transport of photogenerated charge carriers at the Fermi velocity to the electrodes, and interband charge-carrier recombination processes to dominate the ultrafast photocurrent of the CNTs.

KEYWORDS Time-resolved optoelectronic nanoscale transport, carbon nanotubes

Single-walled carbon nanotubes (CNTs) are promising building blocks for future optoelectronic devices because of their compelling electronic and optical properties.^{1–11} So far, only optical methods have been used to characterize the ultrafast dynamics of photogenerated charge carriers in CNTs in the time domain.^{12–17} Typical fluorescence decay times of individual CNTs have been measured to be in the range of tens to hundreds of picoseconds.^{12–16,18} Conventional electronic measurements cannot resolve such ultrafast dynamics because available electronic equipment cannot produce trigger signals and detect transients faster than tens of picoseconds. Furthermore, CNTs typically exhibit a high impedance of several kilohms, and ultrafast charge-carrier dynamics are therefore obscured by the response time of the high-frequency circuits. Here, we introduce an experimental on-chip scheme to measure the photocurrent dynamics of electrically contacted nanosystems in the time domain. The technique applies an ultrafast optical pump–probe scheme to a coplanar stripline circuit, and the photocurrent response of CNTs is sampled by Auston switches.¹⁹ A related terahertz time-domain measurement technique was developed by McEuen et al. to determine the ultrafast electrical response of CNTs.³ While this technique focuses on electrical excitations of the CNTs, the technique presented in this work utilizes an optical laser excitation of the CNTs. The presented optoelectronic scheme, due to its high sensitivity, can follow the dynamics of photogenerated charge carriers on the picosecond time scale. Generally, photocreated excitons in CNTs can be

dissociated by electric fields generated by a large bias voltage,^{2,4,21} at defect sites,⁵ and in the vicinity of Schottky barriers.^{5,11} So far, time-integrated optoelectronic experiments have revealed that hereby a photocurrent^{5,11} and a photovoltage⁵ can originate.² At large bias, energetic carriers in CNTs can also excite optical phonons²² and cause a nonequilibrium phonon distribution.² The latter can give rise to a phonon-assisted dissociation of excitons¹⁷ and to bolometric photoconductance phenomena.^{6,8,9} Our data demonstrate that a combination of an optically induced ultrafast displacement current, transport of photogenerated charge carriers at the Fermi velocity to the electrodes, and interband charge-carrier recombination processes dominate the ultrafast optoelectronic response of the CNTs. A detailed understanding of such ultrafast charge carrier dynamics will become essential to design and build optoelectronic detectors and high-frequency electronic circuits based upon CNTs.²⁰ Our results show that CNTs can act as nanoscale, ultrafast photoswitches in electronic terahertz circuits with a picosecond switching time.

The studied CNTs are grown via an electric-field-assisted chemical vapor deposition method, as described elsewhere²³ and in the Supporting Information, such that a network of CNTs spans two electrodes of a stripline (Figure 1a). The freely suspended CNTs and the two electrodes form a two-terminal stripline circuit driven by a bias voltage V_{SD} (Figure 1b). Temperature-dependent measurements show that the conductance of the CNT network without illumination is dominated by metallic CNTs with semiconducting CNTs acting as tunneling barriers²⁴ (see Supporting Information). Such CNT networks have recently been exploited to

* To whom correspondence should be addressed. holleitner@wsi.tum.de.

Received for review: 10/21/2010

Published on Web: 12/10/2010

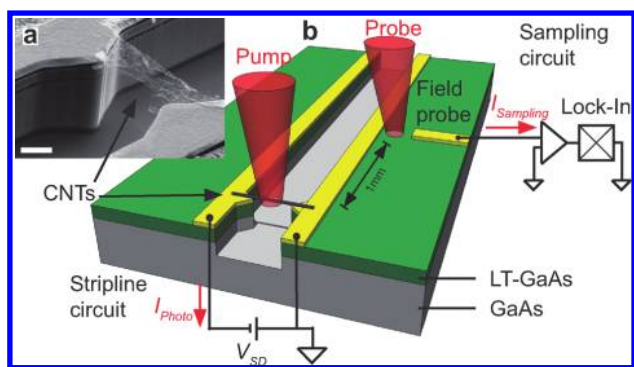


FIGURE 1. Device geometry and optoelectronic pump-probe circuit. (a) Scanning electron microscope (SEM) image of freely suspended single-walled carbon nanotubes (CNTs) spanning two gold electrodes. Scale bar, 3 μm . (b) Schematic on-chip detection geometry. The pump laser pulse is focused on the CNTs contacted by the stripline circuit. The probe-pulse triggers the sampling circuit. Gold electrodes are depicted in yellow.

build biosensors,²⁵ transparent electrodes,²⁶ and bolometric photodetectors.⁶

The suspended CNTs in the stripline circuit are optically excited by a pump-pulse at the second interband transition E_{22} of the semiconducting CNTs in the network with ~ 160 fs pulse length generated by a titanium:sapphire laser (see Supporting Information). After the excitation, an electromagnetic pulse starts to travel along the stripline. A sampling circuit senses the transient electric field of the traveling pulse at the position of a field probe (Figure 1b).²⁷ Here, we utilize an Auston switch¹⁹ based on a low-temperature grown (LT) GaAs substrate. The time delay t_{delay} between the pump and the probe pulse is controlled by a delay stage. Measuring the current I_{Sampling} in the sampling circuit as a function of t_{delay} yields information on the optoelectronic response of the CNTs in the stripline circuit with a picosecond time resolution.²⁷

We first measure the time-integrated, spatially resolved photocurrent I_{Photo} of the freely suspended CNTs in the stripline circuit^{5,11} (Figure 2). At zero V_{SD} , we find two spatial extrema of I_{Photo} , each of which is in the vicinity of an electrode (Figure 2b). The extrema are consistent with intrinsic potential differences between semiconducting CNTs and the metal electrodes^{5,11} in combination with tube-tube junctions between semiconducting and metallic CNTs. In electrostatically undoped CNTs (we apply no back-gate voltage), the Fermi energy can be assumed to lie in the band gap of the CNTs.²⁹ Therefore, the Fermi energy varies strongly with a voltage bias applied across the CNT network. In turn, at large V_{SD} , the Fermi energy crosses from n to p type in between the two electrodes, and a larger fraction of the voltage drop occurs within the CNT network instead of at the contacts. This explains that at $V_{\text{sd}} = -1$ V (+1 V) only one minimum (maximum) of I_{Photo} is observed (Figure 2, panels a and c). Then excitons are dissociated by the large electric fields in the middle of the CNT network and, in turn, they contribute to the time-integrated photocurrent I_{Photo} .^{2,4}

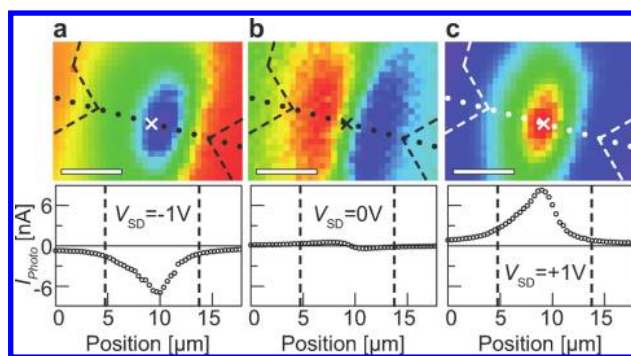


FIGURE 2. Time-integrated photocurrent maps of the CNTs measured in the stripline circuit. (a) Spatially resolved, time-integrated photocurrent I_{Photo} of the CNTs at a bias voltage $V_{\text{SD}} = -1$ V and laser power $P_{\text{Laser}} = 100 \mu\text{W}$. Dashed lines indicate the position of the electrodes. Dotted line depicts the shortest distance, $d = 9 \mu\text{m}$, between the electrodes. (b, c) Equivalent data for $V_{\text{SD}} = 0$ V and +1 V. Scale bars, 5 μm . The lower insets depict line cuts along the dotted lines.

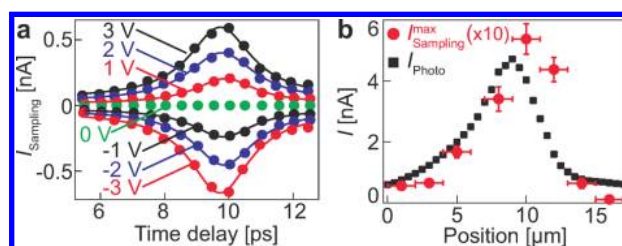


FIGURE 3. Comparison of the time-resolved with the time-integrated photocurrent of the CNTs. (a) Photocurrent signal I_{Sampling} at the sampling circuit for a time delay $t_{\text{delay}} \leq 13$ ps. The pump laser beam is focused at the position marked with a cross in Figure 2 ($-3 \text{ V} \leq V_{\text{SD}} \leq 3 \text{ V}$, $P_{\text{Laser}} = 200 \mu\text{W}$). (b) I_{Sampling} and I_{Photo} as a function of the distance along the direction indicated by the dotted lines in Figure 2 ($V_{\text{SD}} = 3 \text{ V}$, $P_{\text{Laser}} = 200 \mu\text{W}$).

Generally, directly after optical excitation, the photogenerated charge carriers redistribute in order to decrease the local potential differences in the CNT network.^{7,27} This displacement of the charge carriers decreases the electric field E in the irradiated region. In turn, the current density in the CNTs can be described by a transient displacement current density

$$\mathbf{j}_D = \epsilon \epsilon_0 d\mathbf{E}/dt \quad (1)$$

with ϵ and ϵ_0 the relative and vacuum permittivity. For a femtosecond excitation, the displacement current can have a subpicosecond duration, although the carrier lifetime exceeds hundreds of picoseconds.^{27,28}

Figure 3a shows the time-resolved I_{Sampling} as a function of t_{delay} for $|V_{\text{SD}}| \leq 3$ V. For $t_{\text{delay}} \leq 7$ ps, I_{Sampling} equals nearly zero, because during this time delay, the electromagnetic pulse generated at the CNTs has not reached the field probe (see Supporting Information). At $t_{\text{delay}} \sim 10.6$ ps, I_{Sampling} exhibits a first peak with a full width at half-maximum of $w_{1\text{stPeak}} \sim (2.1 \pm 0.1)$ ps. We would like to note the following

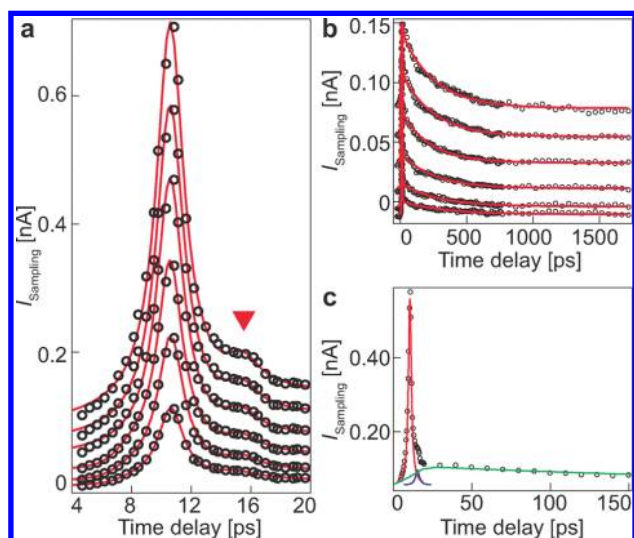


FIGURE 4. Time-resolved photocurrent dynamics of the CNTs. (a) This graph shows I_{Sampling} for t_{Delay} up to 20 ps ($P_{\text{Laser}} = 200 \mu\text{W}$). It exhibits a first and a second peak (triangle), both of which are fitted by Lorentzian functions (lines) ($0.5 \text{ V} \leq V_{\text{SD}} \leq 3 \text{ V}$). (b) I_{Sampling} for t_{Delay} extended to 1.8 ns with fit functions (lines). (c) I_{Sampling} for $V_{\text{SD}} = 2.5 \text{ V}$ and the individual components of the fit function (lines). The first and the second peak are fitted by Lorentzians depicted in red and blue. The slow decay is fitted by an exponentially convoluted Gaussian function with fitting parameter τ_{Slow} , depicted in green.

points. First, the sign of the time-resolved I_{Sampling} can be tuned by V_{SD} , and it directly corresponds to the one of the time-integrated I_{Photo} . Second, both signals vary in the same manner as a function of the position of the pump laser, when it is scanned between the two electrodes (Figure 3b). Hereby, I_{Sampling} is proportional to the electric potential landscape within the CNTs. Therefore, we interpret the first peak of I_{Sampling} to result from an optically induced displacement current,^{27,28} in accordance with eq 1. We point out that both I_{Photo} and I_{Sampling} depend linearly on the pump-laser power P_{Laser} (data not shown).

As depicted in Figure 4a, we find that I_{Sampling} also exhibits a second peak (triangle). It is delayed by $t_{2\text{ndPeak}} = (4.8 \pm 0.2) \text{ ps}$ with respect to the first peak at $\sim 10.6 \text{ ps}$. Such a second peak results from the transport of photogenerated charge carriers to the electrodes, as we recently demonstrated for GaAs in a similar stripline configuration.²⁷ In the present experiment, the laser spot is located in the center between the two electrodes. Therefore, the photogenerated charge carriers in the CNTs need to propagate $d/2 \approx (4.5 \pm 0.5) \mu\text{m}$, before they reach the metal contacts. Assuming an average group velocity of the photogenerated charge carriers in the CNT network, we can estimate its value to be $v_{\text{Group}} = d/(2t_{2\text{ndPeak}}) \sim (0.9 \pm 0.1) \times 10^6 \text{ ms}^{-1}$. Within the experimental error, the value does not vary with V_{SD} in our experiment. Generally, the deduced value of v_{Group} is consistent with the Fermi velocity³ in CNTs of $\sim 0.8 \times 10^6 \text{ ms}^{-1}$. Furthermore, the value is significantly less than the propagation velocity $v_{\text{Plasmon}} = 2.7 \times 10^6 \text{ ms}^{-1}$ of plasmon modes in CNTs.³ Hereby, the measurements suggest that single elec-

tron excitations and not plasmon modes dominate the ultrafast optoelectronic response of freely suspended CNTs.

As can be seen in Figure 4b, I_{Sampling} also exhibits a slow decay component. We utilize the sum of two Lorentzian functions and an exponentially convoluted Gaussian to account for all features in I_{Sampling} . The individual fit functions are plotted in Figure 4c. A fitting parameter τ_{Slow} describes the exponential decay of the convoluted Gaussian, and it can be associated with the slow decay. We find a value of $\tau_{\text{Slow}} = 248 \pm 2 \text{ ps}$, independent of V_{SD} . We note that such a large value of τ_{Slow} is not present when a LT-GaAs substrate substitutes the CNTs in the stripline circuit.²⁷ Following the work by Auston,¹⁹ we interpret τ_{Slow} to be the lifetime of photogenerated charge carriers in the CNT network.¹⁸ We stress that it is outstanding to measure carrier lifetimes in freely suspended, chemical vapor deposition grown CNTs, because such CNTs have a typical interband transition energy E_{11} below 1 eV.^{1,2} This energy range lacks a sufficiently fast photodetector. On top, our on-chip detection scheme resolves the transport and photocurrent dynamics in electronically contacted CNTs. Finally, we would like to note that the scheme is sensitive enough to measure the charge carrier dynamics in single semiconducting and metallic CNTs.

In conclusion, we present an optoelectronic measurement scheme with picosecond time resolution, allowing time-dependent photocurrent studies of electrically contacted nanosystems. In particular, we demonstrate that the ultrafast photocurrent response of CNTs comprises a displacement current and a transport current and that CNT networks can be exploited as ultrafast photodetectors with a switching time in the picosecond time scale. The data further suggest that the photocurrent is finally terminated by the recombination lifetime of the charge carriers. The versatility of the presented optoelectronic technique recommends further time-domain experiments with picosecond resolution on electrically contacted nanoscale systems, such as graphene,³⁰ quantum wires, and nanowires.³¹

Acknowledgment. We thank J. P. Kotthaus, A. Hartschuh, G. Abstreiter, and M. Mangold for fruitful discussions and I. Zardo, M. Kaniber, and A. Laucht for technical help. We gratefully acknowledge financial support from the DFG, the Center for NanoScience (CeNS), and the German excellence initiative via the “Nanosystems Initiative Munich (NIM)” and “LMUexcellent”. L.S. thanks the Alexander von Humboldt foundation for support.

Supporting Information Available. Details on the LT-GaAs-heterostructure, the coplanar stripline circuit, the sample preparation, the electronic and optical properties of the CNTs, the dispersion of the coplanar striplines, and further control experiments. This material is available free of charge via the Internet at <http://pubs.acs.org>.

REFERENCES AND NOTES

- (1) *Carbon Nanotubes: Advanced Topics in the Synthesis, Structure, Properties and Applications*; Jorio, A., Dresselhaus, M. S., Dresselhaus, G., Eds.; Springer: Berlin, Heidelberg, 2008.
- (2) Avouris, Ph.; Freitag, M.; Perebeinos, V. *Nat. Photonics* **2008**, *2*, 341.
- (3) Zhong, Z.; Gabor, N. M.; Sharping, J. E.; Gaeta, A.; McEuen, P. L. *Nat. Nanotechnol.* **2008**, *3*, 201.
- (4) Freitag, M.; Martin, Y.; Misewich, J. A.; Martel, R.; Avouris, P. *Nano Lett.* **2003**, *3*, 1067.
- (5) Balasubramanian, K.; Burghard, M.; Kern, K.; Scolari, M.; Mews, A. *Nano Lett.* **2005**, *5*, 507.
- (6) Itkis, M. E.; Borondics, F.; Yu, A.; Haddon, R. C. *Science* **2006**, *312*, 415.
- (7) Mohite, A.; Lin, J.-T.; Sumanasekera, G.; Alphenaar, B. W. *Nano Lett.* **2006**, *6*, 1369.
- (8) Tsen, A. W.; Donev, L. A. K.; Kurt, H.; Herman, L. H.; Park, J. *Nat. Nanotechnol.* **2009**, *4*, 108.
- (9) Zebli, B.; Vieyra, H. A.; Carmeli, I.; Hartschuh, A.; Kotthaus, J. P.; Holleitner, A. W. *Phys. Rev. B* **2009**, *79*, 205402-1.
- (10) Carmeli, I.; Mangold, M.; Frolov, L.; Zebli, B.; Carmeli, Ch.; Richter, S.; Holleitner, A. W. *Adv. Mater.* **2007**, *19*, 3901.
- (11) Kaniber, S.; Song, L.; Kotthaus, J. P.; Holleitner, A. W. *Appl. Phys. Lett.* **2009**, *94*, 261106.
- (12) Ostojic, G. N.; Zaric, S.; Kono, J.; Strano, M. S.; Moore, V. C.; Hauge, R. H.; Smalley, R. E. *Phys. Rev. Lett.* **2004**, *92*, 117401.
- (13) Ma, Y.-Z.; Stenger, J.; Zimmermann, J.; Bachilo, S. M.; Smalley, R. E.; Weismann, R. B.; Fleming, G. R. *J. Chem. Phys.* **2004**, *120*, 3368.
- (14) Huang, L.; Pedrosa, N.; Krauss, T. D. *Phys. Rev. Lett.* **2004**, *93*, 017403-1.
- (15) Wang, F.; Dukovic, G.; Brus, L. E.; Heinz, T. F. *Phys. Rev. Lett.* **2004**, *92*, 177401-1.
- (16) Hagen, A.; Steiner, M.; Raschke, M. B.; Lienau, C.; Hertel, T.; Qian, H.; Meixner, A. J.; Hartschuh, A. *Phys. Rev. Lett.* **2005**, *95*, 197401-1.
- (17) Perebeinos, V.; Avouris, P. *Phys. Rev. Lett.* **2008**, *101*, 057401-1.
- (18) Perebeinos, V.; Tersoff, J.; Avouris, P. *Nano Lett.* **2005**, *5*, 2495-2499.
- (19) Auston, D. H. *IEEE J. Quantum Electron.* **1983**, *19*, 639.
- (20) Rutherglen, C.; Jain, D.; Burke, P. *Nat. Nanotechnol.* **2009**, *4*, 811.
- (21) Perebeinos, V.; Avouris, P. *Nano Lett.* **2007**, *7*, 609.
- (22) Yao, Z.; Kane, C. L.; Dekker, C. *Phys. Rev. Lett.* **2000**, *84*, 2941.
- (23) Song, L.; Holleitner, A. W.; Qian, H.; Hartschuh, A.; Döblinger, M.; Weig, E. M.; Kotthaus, J. P. *J. Phys. Chem. C* **2008**, *112*, 9644.
- (24) Kaiser, A. B.; Düsberg, G.; Roth, S. *Phys. Rev. B* **1998**, *57*, 1418.
- (25) Snow, E. S.; Perkins, F. K.; Houser, E. J.; Badescu, S. C.; Reinecke, T. L. *Science* **2005**, *307*, 1941.
- (26) Wu, Z.; Chen, Z.; Du, X.; Logan, J. M.; Sippel, J.; Nikolou, M.; Kamaras, K.; Reynolds, J. R.; Tanner, D. B.; Hebard, A. F.; Rinzler, A. G. *Science* **2004**, *305*, 1273.
- (27) Prechtel, L.; Manus, S.; Schuh, D.; Wegscheider, W.; Holleitner, A. W. *Appl. Phys. Lett.* **2010**, *26*, 261110-1.
- (28) Krökel, D.; Grischkowsky, D.; Ketchen, M. B. *Appl. Phys. Lett.* **1989**, *54*, 1046.
- (29) Bushmaker, A. W.; Deshpande, V. V.; Hsieh, S.; Bockrath, M. W.; Cronin, S. B. *Nano Lett.* **2009**, *9*, 2862.
- (30) Mueller, T.; Xia, F.; Avouris, P. *Nat. Photonics* **2010**, *4*, 297.
- (31) Thunich, S.; Prechtel, L.; Spirkoska, D.; Abstreiter, G.; Fontcuberta i Morral, A.; Holleitner, A. W. *Appl. Phys. Lett.* **2009**, *95*, 083111.